Supporting information

Flexible organic crystal-quantum dot hybrids with adjustable waveguides

General information

Scanning electron microscopy (SEM) images were obtained on the FEI Quanta 450 operated at 5–10 kV. UV−vis absorption spectra were recorded by a Shimadzu UV-2550 spectrophotometer. The emission spectra were recorded on a Maya2000 Pro CCD spectrometer. For the optical waveguide text, the crystals were irradiated by the third harmonic (355 nm) of a Nd:YAG (yttrium-aluminum-garnet) laser at a repetition rate of 10 Hz and a pulse duration of about 10 ns. The energy of laser was adjusted by using the calibrated neutral density filters. The beam was focused on a stripe whose shape was adjusted to 3.3 × 0.6 mm by using a cylindrical lens and a slit. The edge emission spectra were recorded on a Maya2000 Pro CCD spectrometer. All solvents and starting materials for syntheses were purchased from commercial sources and were used as received without further purification. Poly(diallyldimethylammonium chloride) (PDDA, Mw. 200000–350000), poly(sodium styrene sulfonate) (PSS, Mw. 70000). PDDA and PSS aqueous solutions were at a concentration of 1.0 mg/mL.

Preparation of crystals 1–4

A dichloromethane solution of compounds **1**–**4** was placed in a test tube. About two times the volume of ethanol was then added along the wall of the test tube without affecting the surface of the solution and keeping the solution undisturbed to allow diffusion to occur. Needle crystals of compound **1**–**4** were obtained after one to two weeks at room temperature.

Supplementary figures

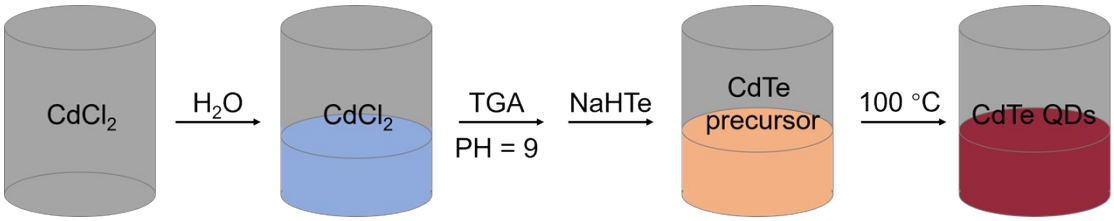

Figure S1. Preparation of aqueous QDs. The procedure for synthesizing CdTe QDs in aqueous media. Preparation process of CdTe quantum dots: Firstly, $CdCl_2$ powder was dissolved in water to form an aqueous solution with a concentration of 1.25×10^{-3} N. Then the pH value of the solution was adjusted to 9.0 and thioglycolic acid (TGA) was added as a stabilizer. The NaHTe solution was then added to the pH-adjusted $CdCl_2$/TGA mixture under nitrogen protection to form a CdTe precursor solution with a fixed molar ratio of Cd^{2+}/ TGA /HTe^- of 1:2.4:0.5. The resulting mixture was heated up to 100°C to initiate and control the growth of CdTe quantum dots. CdTe nanoparticles with different luminescent colors were obtained by adjusting the reaction time at this temperature.

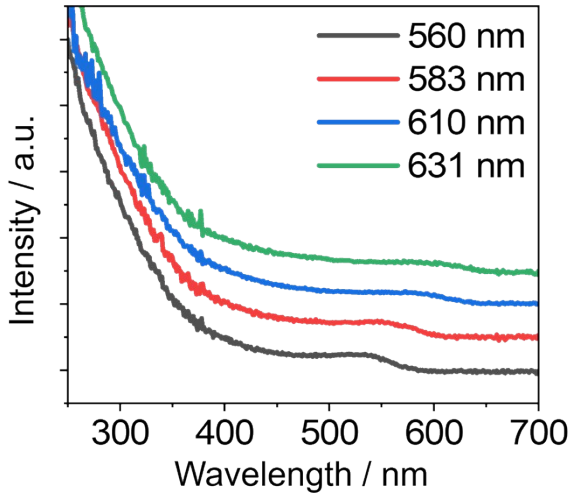

Figure S2. Absorption spectra of aqueous QDs. Absorption spectra of the aqueous solutions of CdTe QDs, which correspond to the PL emission centered at 560, 583, 610, and 631 nm, respectively.

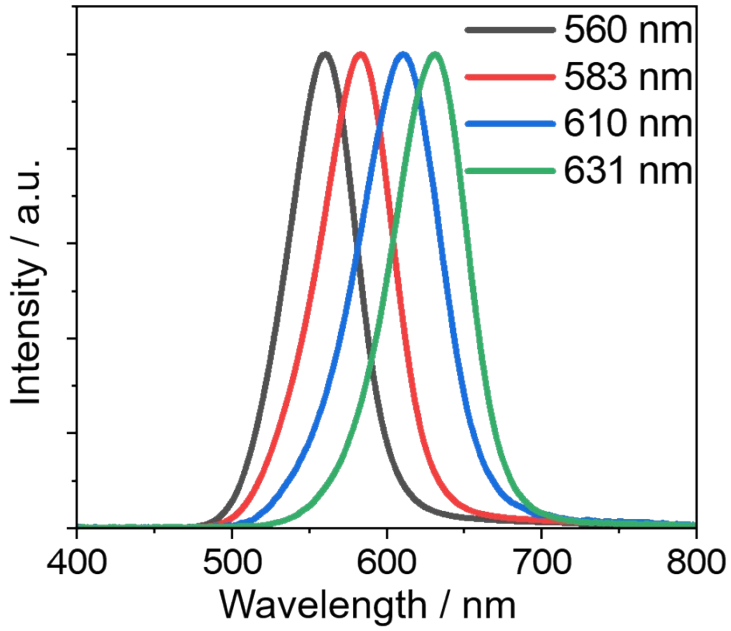

Figure S3. PL Emission spectra of aqueous QDs. Emission spectra of the aqueous solutions of four CdTe QDs with the emission peaks at 560, 583, 610, and 631 nm, respectively.

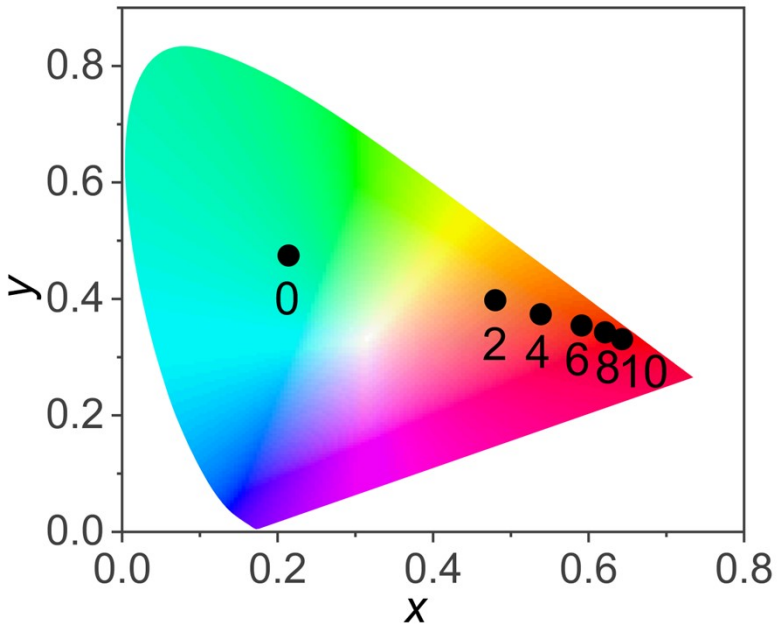

Figure S4. CIE Coordinate Chart. CIE coordinate plots illustrating the Q//**1** spectrum in relation to the count of CdTe QD layers are presented.

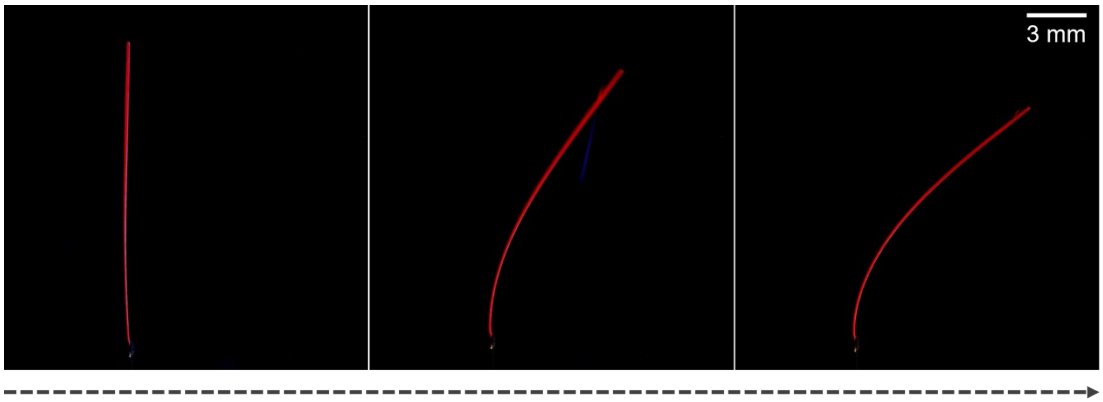

Figure S5. Images of hybrid materials. Photographs of Q//**3** (red) bending.

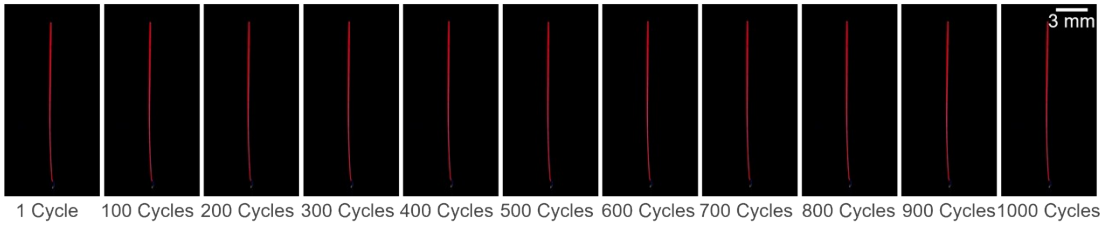

Figure S6. Durability experiments on hybrid materials. Photographs of Q//**3** (red) after repeated bending.

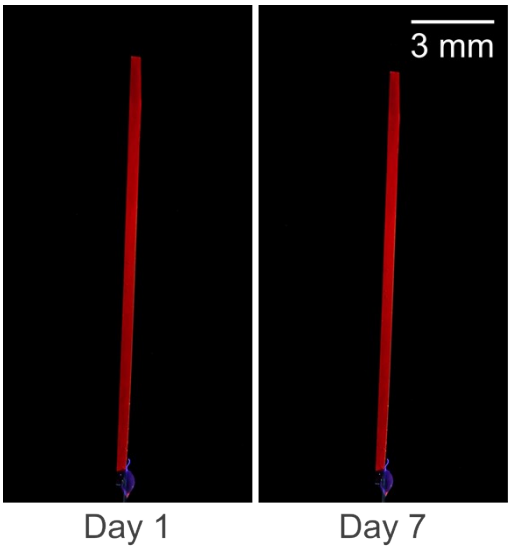

Figure S7. Durability experiments on hybrid materials. Photographs of Q//**3** (red) after being placed for a long period of time.

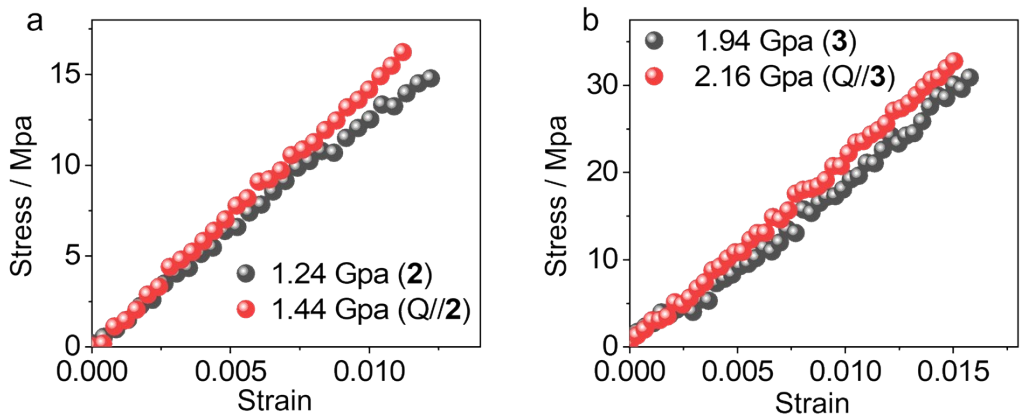

Figure S8. Mechanical property test of crystals. (a) Crystal **2** and Q//**2**. (b) Crystal **3** and Q//**3**.

Figure S9. Preparation of hybrid materials. Photographs of large-volume automated preparation of hybrid materials on coater.

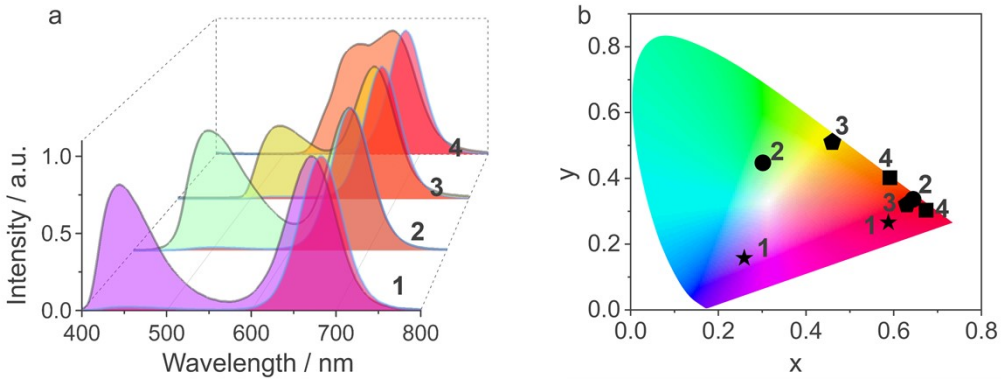

Figure S10. Control of the length of CdTe coatings on crystal surfaces. (a) Spectral data pertaining to the crystals (The blue boxes delineated the optical signals corresponding to the position of the CdTe coating, while the black boxes signify the optical signals observed at the intersection of the CdTe coating and PDDA/PSS//**1**–**4**). (b) CIE coordinate plots showcasing the spectra of Q//**1**–**4**.

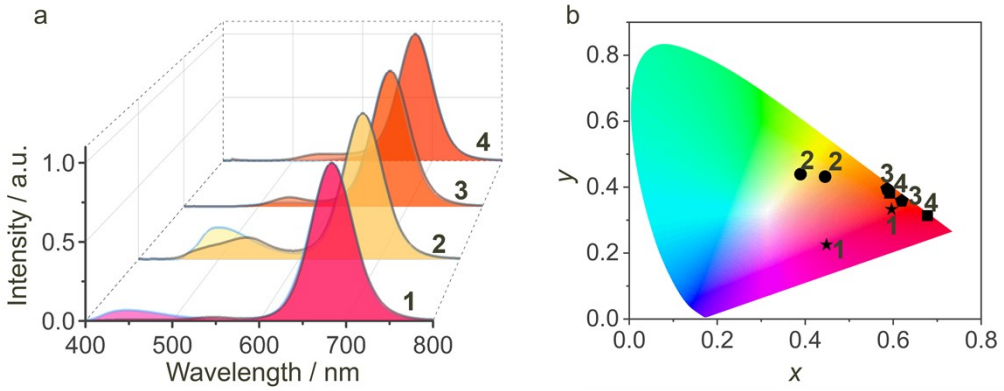

Figure S11. Control of the length of CdTe coatings on crystal surfaces. (a) Spectral data pertaining to the crystals (The black boxes signify the optical signals corresponding to the points of overlap between the yellow and red CdTe coatings, while the blue boxes indicate the optical signals corresponding to the positions solely occupied by the red CdTe coating). (b) CIE coordinate plots showcasing the spectra of Q//**1**–**4**.

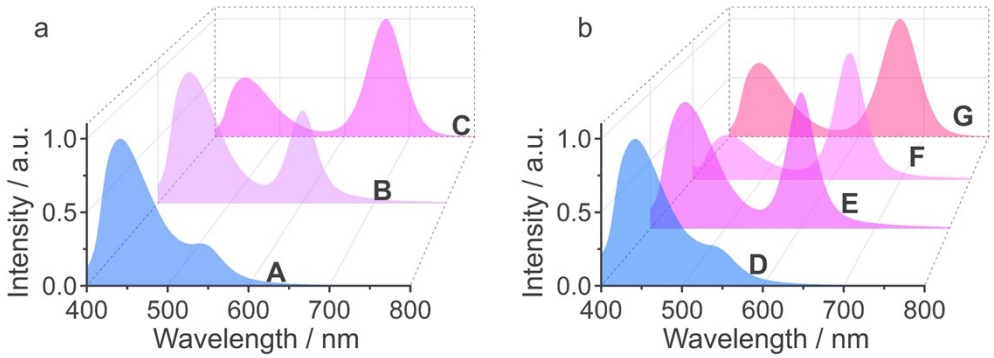

Figure S12. Emission spectra of hybrid materials. (a) The spectral data of the Q//**1** (**A**, **B** and **C**). (b) The spectral data of the Q//**1** (**D**, **E**, **F** and **G**).

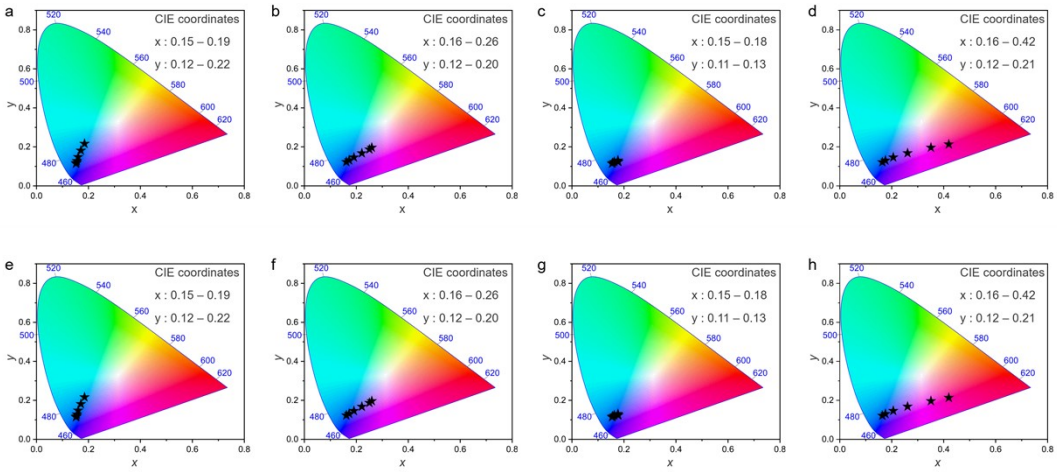

Figure S13. CIE Coordinate Plots of hybrid materials. (a–d) The CIE coordinate plots depicting the spectra of Q//**1** were showcased in panels a (green), b (yellow), c (orange), and d (red), which correspond to Figure 4e. (e–h) The CIE coordinate plots depicting the spectra of Q//**1** were showcased in panels e (green), f (yellow), g (orange), and h (red), which correspond to Figure 4f.

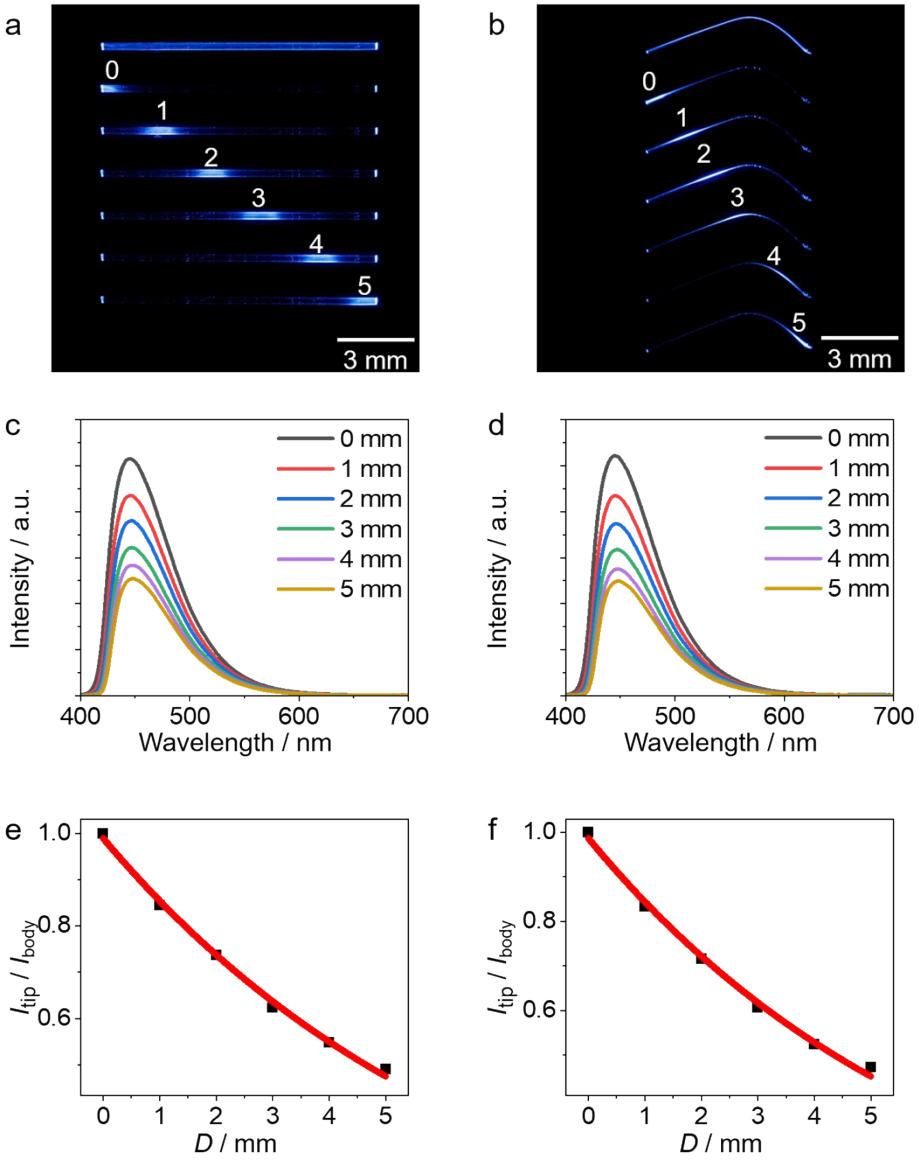

Figure S14. Optical waveguide experiment. (a,b) Image of crystal **1** used as a waveguide, (a) Crystal **1** in straight state, (b) Crystal **1** in straight state. (c,d) Fluorescence spectra were collected at the fixed end of the crystal, while the crystals were exited at different position by 355 nm laser, position differences between the fixed end and the excitation position is defined as distance (mm). The panels c and d are corresponding to the crystals shown in panels a and b, respectively. (e,f) Decay of intensity with distance I_{tip}/I_{body}. The optical loss coefficient (α) is obtained by a single exponential fitting function. $I_{tip}/I_{body} = A\exp(-\alpha D)$, in which I_{tip} and I_{body} are the fluorescence intensities measured at the fixed end and the excitation position, respectively. A is the optical loss coefficient and D is position differences between the fixed end and the excitation position. (e) Crystal **1**. in straight state, (f) Crystal **1**. in bent state.

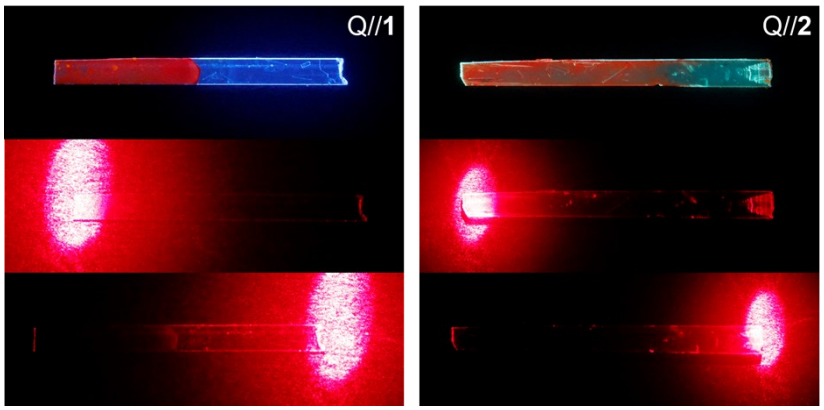

Figure S15. Optical waveguide experiment. Photographs of crystal Q//**1**,**2** for passive optical signal transmission.

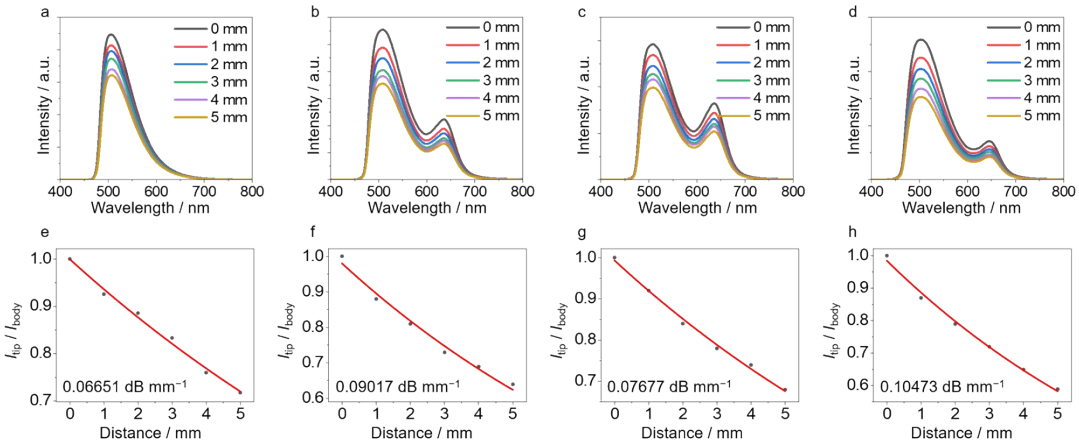

Figure S16. Optical waveguide experiment. (a-d) Fluorescence spectra were collected at the fixed end of the crystal, while the crystals were exited at different position by 355 nm laser, position differences between the fixed end and the excitation position is defined as distance (mm), crystal **2** (a), sample 1 of Q//**2** (b), sample 2 of Q//**2** (c), and sample 3 of Q//**2** (d). (e,f) Decay of intensity with distance I_{tip}/I_{body}. The optical loss coefficient (α) was obtained by a single exponential fitting function. $I_{tip}/I_{body} = A\exp(-\alpha D)$, in which I_{tip} and I_{body} were the fluorescence intensities measured at the fixed end and the excitation position, respectively. A was the optical loss coefficient and D was position differences between the fixed end and the excitation position. crystal **2** (e), sample 1 of Q//**2** (f), sample 2 of Q//**2** (g), and sample 3 of Q//**2** (h).

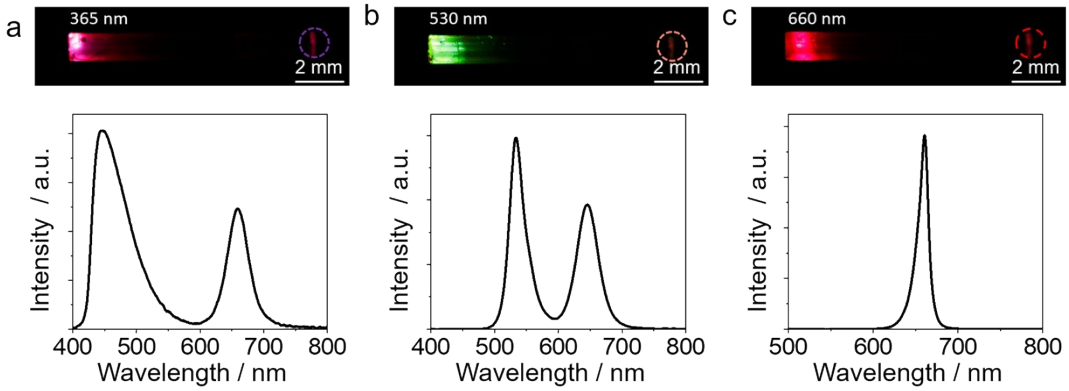

Figure S17. Wavelength dependence of hybrid materials. (a) Optical signal transmission image and right reception spectrum when Q//**1** was excited by a 365 nm light source. (b) Optical signal transmission image and right reception spectrum when Q//**1** was excited by a 530 nm light source. (c) Optical signal transmission image and right reception spectrum when Q//**1** was excited by a 660 nm light source.

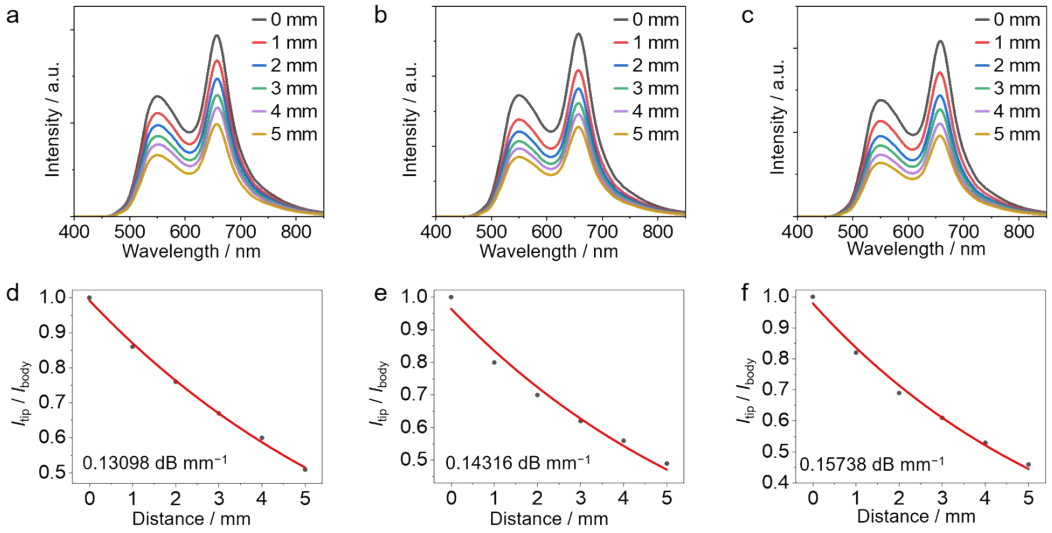

Figure S18. Optical waveguide experiment. (a-c) Fluorescence spectra were collected at the fixed end of the crystal, while the crystals were exited at different position by 355 nm laser, position differences between the fixed end and the excitation position is defined as distance (mm), Q//**3** bending 0 times (a), Q//**3** bending 500 times (b), and Q//**3** bending 1000 times (c). (d-f) Decay of intensity with distance I_{tip}/I_{body}. The optical loss coefficient (α) was obtained by a single exponential fitting function. $I_{tip}/I_{body} = A\exp(-\alpha D)$, in which I_{tip} and I_{body} were the fluorescence intensities measured at the fixed end and the excitation position, respectively. A was the optical loss coefficient and D was position differences between the fixed end and the excitation position. Q//**3** bending 0 times (d), Q//**3** bending 500 times (e), and Q//**3** bending 1000 times (f).

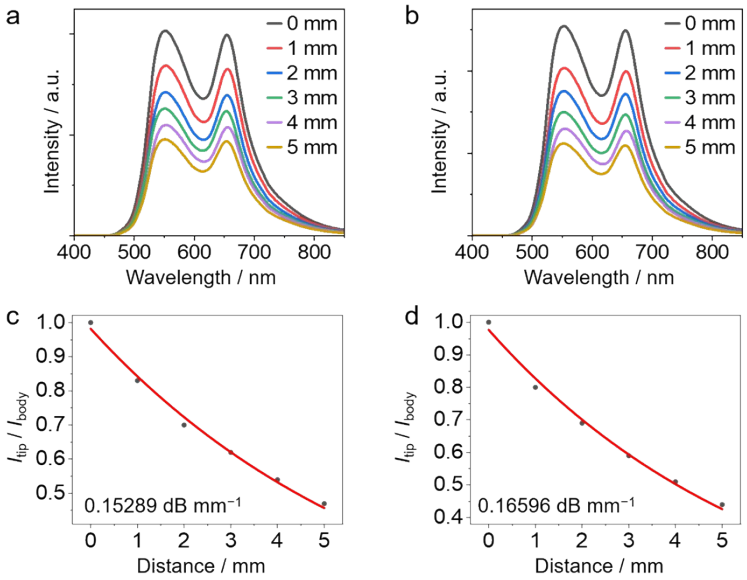

Figure S19. Optical waveguide experiment. (a,b) Fluorescence spectra were collected at the fixed end of the crystal, while the crystals were exited at different position by 355 nm laser, position differences between the fixed end and the excitation position is defined as distance (mm), Q//**3** original state (a) and Q//**3** placed for 7 days (b). (c,d) Decay of intensity with distance I_{tip}/I_{body}. The optical loss coefficient (α) was obtained by a single exponential fitting function. $I_{tip}/I_{body} = A\exp(-\alpha D)$, in which I_{tip} and I_{body} were the fluorescence intensities measured at the fixed end and the excitation position, respectively. A was the optical loss coefficient and D was position differences between the fixed end and the excitation position. Q//**3** original state (c) and Q//**3** placed for 7 days (d).

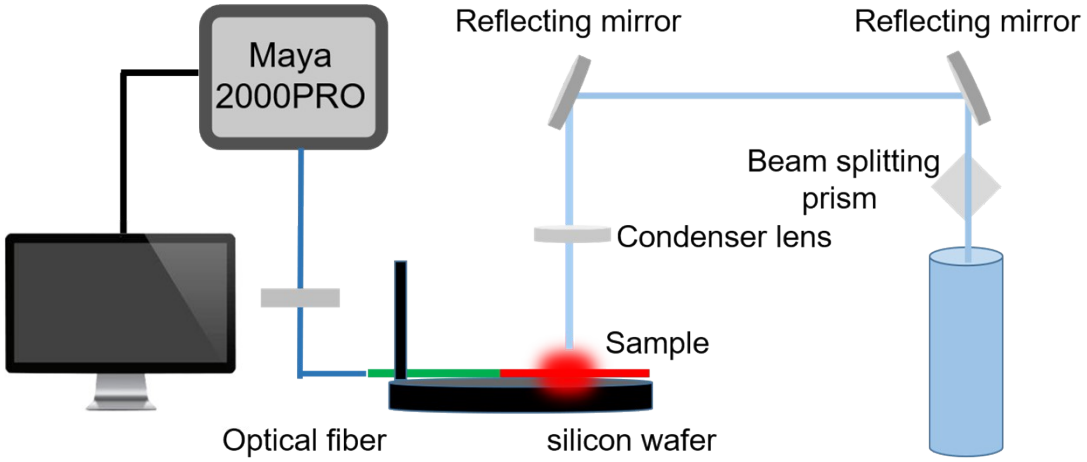

Figure S20. Diagram depicting the experimental for secure transmission of encrypted information. Schematic illustrating the experimental configuration for information encryption trials involving hybridized materials, with the color red denoting the area for the QD coating.

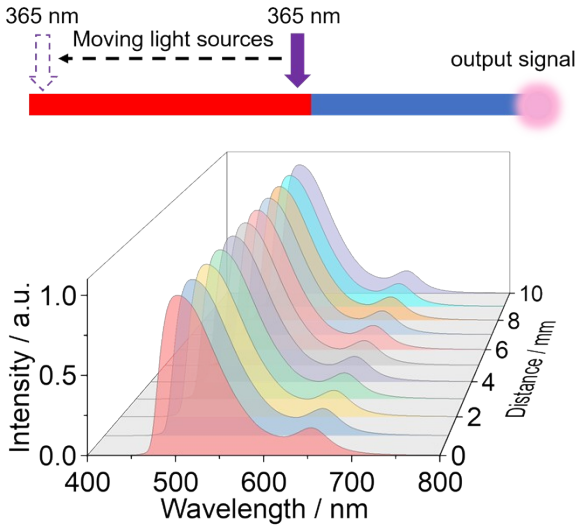

Figure S21. Optical signal transmission of hybrid materials. Spectral signals when the excitation light source was located at different quantum dot coating positions of Q//**2**.

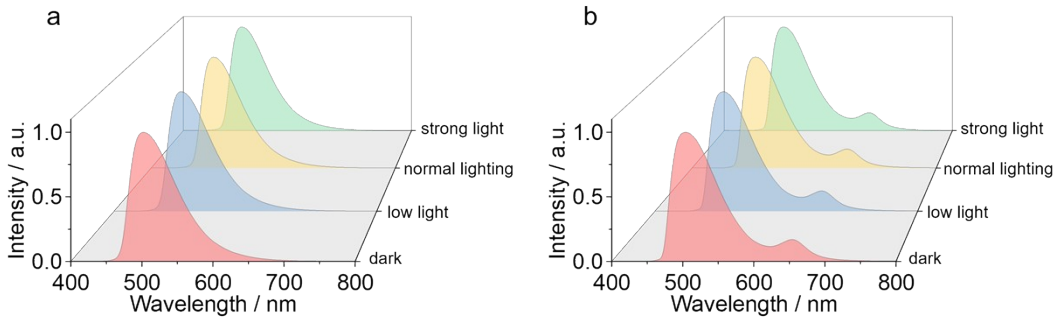

Figure S22. Optical signal transmission of hybrid materials. (a-b) Spectral signals of the hybrid material placed under different ambient light conditions (dark, low light, normal lighting, strong light), signal “0” (a), signal “1” (b).

Supplementary Table

Table S1. Table of optical loss coefficients for hybrid organic crystals and state-of-the-art optical waveguide materials.

Optical waveguide material	**DMDAT**	**CTVB**	**Cz-2CF$_3$**	**DPTPD**	**P-1**	**HDBP**	**This work**
Optical loss coefficient	0.144 dB mm^{-1}	2.157 dB mm^{-1}	0.0757 dB μm^{-1}	0.136 dB mm^{-1}	0.058 dB mm^{-1}	0.125 dB mm^{-1}	0.090 dB mm^{-1}

Table S2. Table of optical loss coefficients for hybrid organic crystals and state-of-the-art optical waveguide materials.

Letter	Binary Code	Letter	Binary Code	Letter	Binary Code
A	01000001	J	01001010	S	01010011
B	01000010	K	01001011	T	01010100
C	01000011	L	01001100	U	01010101
D	01000100	M	01001101	V	01010110
E	01000101	N	01001110	W	01010111
F	01000110	O	01001111	X	01011000
G	01000111	P	01010000	Y	01011001
H	01001000	Q	01010001	Z	01011010
I	01001001	R	01010010		